IEEE Access
Multidisciplinary | Rapid Review | Open Access Journal

SPECIAL SECTION ON ANTENNA AND PROPAGATION FOR 5G AND BEYOND

Received September 1, 2019, accepted September 10, 2019, date of publication September 17, 2019,
date of current version September 30, 2019.

Digital Object Identifier 10.1109/ACCESS.2019.2941908

Eight Element Multiple-Input Multiple-Output (MIMO) Antenna for 5G Mobile Applications

MUJEEB ABDULLAH[1], SAAD HASSAN KIANI[2], AND AMJAD IQBAL[3], (Student Member, IEEE)

[1]Department of Computer Science, Bacha Khan University, Charsadda 24420, Pakistan
[2]Electrical Engineering Department, Iqra National University, Peshawar 2500, Pakistan
[3]Centre for Wireless Technology, Faculty of Engineering, Multimedia University, Cyberjaya 63100, Malaysia

Corresponding author: Amjad Iqbal (amjad730@gmail.com)

ABSTRACT This work presents a systematic design of high performance eight element antenna array for a 5G mobile terminal operating at 2.6/3.5 GHz bands. The proposed eight element slot antenna array based on unit monopole slot antenna embedded in the metal casing or ground resonates at fundamental mode at 2.6 GHz. The antenna array is developed from four antennas (open-end slot antenna) etched near to the corner edges of the printed circuited board with supported pairs of vertically mounted slot antennas in middle section of the long edge ground plane. This combination of the antenna elements provided pattern diversity and enabled the smartphone in the reception of the signal in a different direction. The impedance bandwidth based on -10 dB return loss criteria cover from 2.4 GHz to 3.6 GHz includes the two allocated bands of (2400 MHz to 2600 MHz) and (3400 MHz to 3600 MHz) for 5G cellular communication systems. The vital MIMO performance measures as envelope correlation coefficient or ECC is less than 0.2 for any two antenna array meeting the required standard of less than 0.5 alongside the mean effective gain or MEG ratio of any two antenna meeting the required standard of less than 3 dB for power balance and optimal diversity performance. As modern smartphone demand desires slim handsets, the after mentioned compact multiple antenna structure can be easily implemented for the future smartphones as it utilizes the conductive sheet or chassis and the middle vertically mounted antenna do not use the additional space of the chassis or ground. The customer hand or human hand effect on the multiple antenna array to mimic the use of mobile phone customer is also studied. The maximum MIMO Channel capacity based on measured result is 34.25bps/Hz and is about 3 times of 2×2 MIMO operations.

INDEX TERMS Channel capacity, envelope correlation coefficient, mean effective gain, mutual coupling, slot antennas, multiple input multiple output.

I. INTRODUCTION

With steadily evolving of communication technology, there is an ever-increasing demand to maximize throughput with available bandwidth. This hardens task is attained by incorporating multiple antenna at the base station also referred as Massive MIMO [1]. On the contrary, accommodating multiple antenna on single printed circuit board is cumbersome and lead to mutual coupling. This interaction leads to a reduction in the efficiency of the antenna and worsens the performance of multiple antenna arrays for MIMO application for which antenna decoupling techniques as discussed in [2] are often used. Also, the smartphone is preferred to be less weight, thin, attractive, as result metal casings have become popular. By using conventional antenna such as a patch antenna, Inverted-F antennas or planar-inverted-F antenna within proximity of metal casing leads to deteriorating radiation efficiency and bandwidth. Therefore, slot antenna embedded in the metal casing can be helpful with good performance regarding bandwidth and radiation efficiency to be used as multiple antenna structures to realize a MIMO system for future 5G smartphone. For future 5G technology providing Mobile broadband service at 2.6 GHz and 3.5 GHz band or also referred below 6 GHz band in [3] are allocated to be used by cellular companies.

The associate editor coordinating the review of this manuscript and approving it for publication was Hassan Tariq Chattha.

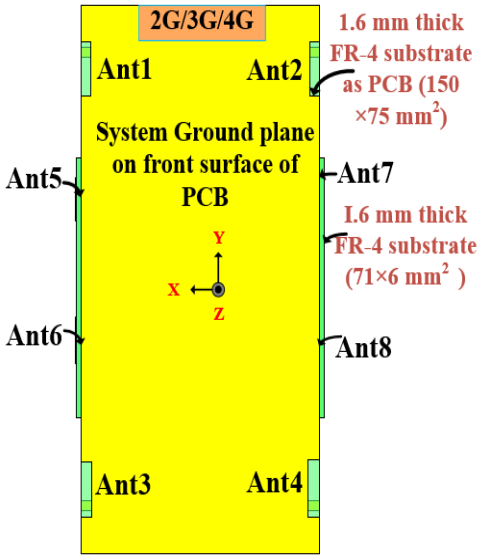

FIGURE 1. Proposed MIMO antenna array.

In the reported work [4]–[8] the multiple antenna arrays for 5G presented for specific frequency band such as in [4] the operating band is 2.4 GHz, in [5], [6] the multiple antenna structure work at 2.6 GHz for MIMO application. The multiple antenna systems at 3.5 GHz also reported in [6] using open-end slot antenna and in [7]–[9] for 3.6 GHz. The other reported mobile antenna structure for MIMO implementation are mentioned in [5]–[7], [10]–[17]. As reported multiple antenna structure for MIMO application vary in geometry and size and mostly support a selective frequency band. On the contrary, in this paper a multiple input multiple output MIMO structure is presented capable of operating at 2.6 and 3.5 GHz bands simultaneously or Wideband MIMO antenna with less complexity helpful to employ intra-band contiguous carrier aggregation to increase the data throughput and applicable to a future 5G smartphone.

II. ANTENNA CONFIGURATION

The detailed procedure to design eight slot antenna structure for implementation of MIMO operation in a smartphone is discussed in this section. Firstly, to swiftly accommodate 2G/3G/4G antenna, space reservation is made by allocating suitable area. The multiple antenna array is designed on the FR-4 substrate with a permittivity of 4.4 which serve as a circuit board with a dimension of 150 × 70 mm^2.

The proposed eight slot antenna array design is based on unit slot antenna, consisting of rectangular open-end slot or monopole slot antenna etched along the different position of ground plane. Four antenna elements (open-end slot antenna) are etched near to the corner edges of the printed circuited board and the middle of each long edge of ground plane supports two slot antenna vertically mounted as illustrated in Fig. 1 in such a way that each open-end slot antenna is fed by inverted L-shaped, microstrip-fed (ILMF) printed on the backside of the substrate as shown in Fig. 2.

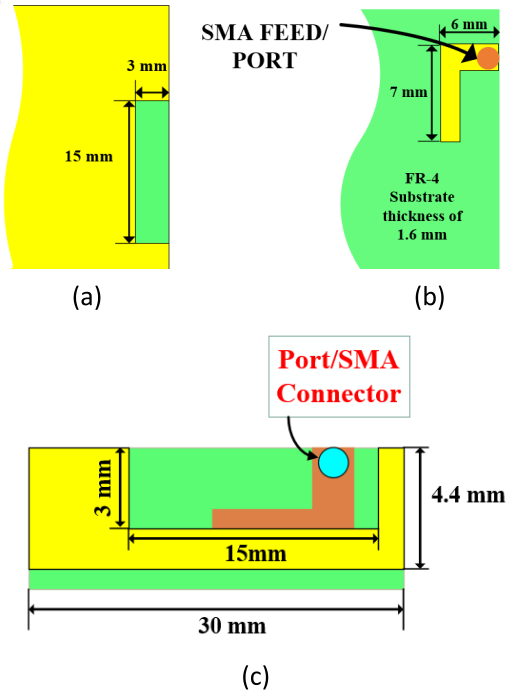

FIGURE 2. Unit slot antenna detail dimensions (a) rectangular-open end slot (b) Inverted-L feeding stripe printed on back side of the ground plane (c) rectangular-open end slot added at the longer edge of the ground plane.

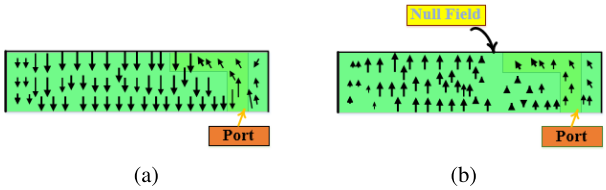

FIGURE 3. Electric field distribution (a) rectangular-open end slot for 2.6 GHz (b) Field distribution at 3.5 GHz showing a factious short along the slot causing the second resonance.

III. PORT EXCITATION MODELING

The off-center inverted L-shape microstrip-fed (ILMF) is used to couple electromagnetic power in the slot. The unit slot antenna resonates at the fundamental resonating frequency of 2.6 GHz. By choosing appropriate microstrip feeding (parallel feed configuration) mechanism or in this case ILMF, the electric field distribution can be modified and create fictitious short circuits along the slot, give rise to the additional resonance of 3.5 GHz besides the main one (2.6 GHz). The fictions short is produced when the slot electric field is effectively canceled by the electric field of the ILMF, previously reported in [18]. The electric field produced due to excitation of the slot is in the opposite direction to the source or ILMF feeding over the area (which does not have ground plane) result in this phenomena.

As shown in Fig. 3b, the null field or factious short circuit produced by ILMF. By properly adjusting the ILMF, the null field or factious short corresponds to second resonance at 3.5 GHz is attained.

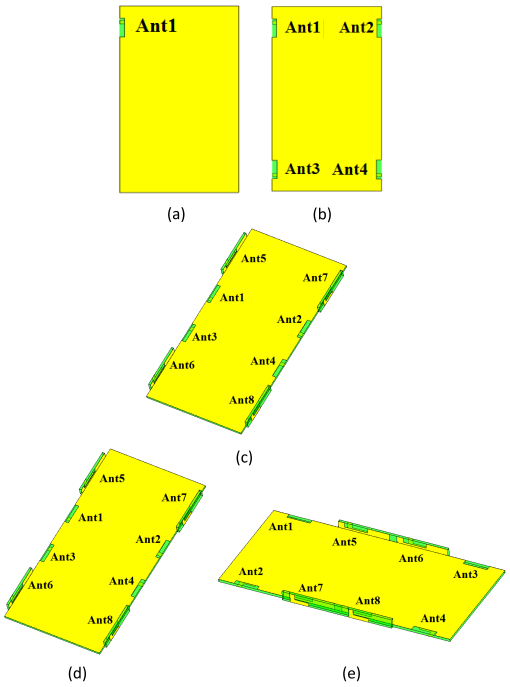

FIGURE 4. Design evolution multiple slot antenna system for MIMO operation with a different combination of the horizontal rectangular slot antenna and vertically mounted slot antenna (a) Single unit slot antenna (b) Four slot antenna etched near to the boundary of the system chassis (c) different combination of horizontal rectangular slot antenna with vertical mounted slot antenna with open-end (d) Case 2 (e) Proposed design.

IV. S-PARAMETER ANALYSIS

Initially, a single open-ended slot antenna with a rectangular shape is etched near to the corner edge of the chassis with scattering parameters obtained using CST Microwave Studio 2019, as shown in Fig. 4a. From S-parameter result, it is evident that the single unit slot antenna can achieve impedance bandwidth covering 2.4 to 3.6 GHz helpful to operate for 2.6 and 3.5 GHz bands for future 5G wireless communication systems as illustrated in Fig. 5a. Then three more open-end slot antenna structure is craved in the system conductive sheet or chassis with signal port excitation already discussed in port modeling. The adding three more open-end slot antenna has less effect on the impedance matching for Ant1 as shown in the S-parameters (Fig. 5b). Naturally, the good isolation between antenna elements is quantified by scattering parameters attain (≤ -15 dB) as inter-spacing between them is greater than $\lambda_g/2$. An attempt is made to mount two vertically mounted open-end slot antenna each along the long edges of the system chassis as demonstrated in Fig. 4a to Fig. 4e. This combination is beneficial because of its ease of integration with a smartphone without any significant modification to the system ground plane. Also owing to the symmetry concerning the middle line of the circuit board the performance of Ant1 and Ant5 are discussed for further study or design of array.

This combination is beneficial because of its ease of integration with a smartphone without any significant modification to the system ground plane. Also owing to the symmetry concerning the middle line of the circuit board the performance of Ant1 and Ant5 are discussed for further study or design of array.

To understand the effect of altering the position of slot antenna with the different combination is studied and classified as Case-1 and Case-2 with corresponding S-parameters as given in Fig. 5c and Fig. 5d respectively. And later, the proposed MIMO antenna array with corresponding S-parameters as shown in Fig. 5e. For Case-1, the resonating frequency of slot antenna Ant1 is shifted with a notch at 3.6 GHz, lack of covering the 2.6 GHz and isolation between antenna elements is better than 10 dB and inter-spacing is greater than half wave-length. As for Case-2, the orientation of the vertically mounted antennas are inverted. And the ILMF of each (Ant1 to Ant4) is moved to the opposite ends. But, it does not bear any significant change in its resonating frequency as shown in Fig. 5d, with minor improvement in impedance matching. Hence, for proposed structure, the vertically mounted slot antennas (Ant1 to Ant5) are shifted to mid-section of the system chassis, and the horizontal slot antenna reverts to original positions as shown in Fig. 5e. As expected the resonating frequency will be shifted as by adding vertically mounted slot antenna along edges, yet it can cover the required band of 2.6/3.5 GHz with good impedance matching. The isolation between Ant1 and Ant5 as quantified by S51 is greater than 13 dB and further improved to 20 dB for 3.5 GHz.

V. MEASURED RESULTS

The proposed antenna array for MIMO operation is fabricated as depicted in Fig. 6. The measurement of scattering parameters is performed with the aid of Agilent Network analyzer N5247A. The 2-D far-field measurements are carried out in an anechoic chamber. The measured results are depicted in Fig. 7-Fig. 10. The simulated result agrees well with the measured result for Ant1 and Ant5 with slight shift may attribute to SMA connector effect as shown in Fig. 10a. From the measured S-parameter result the Ant1 and Ant5 able to operate at 2.6/3.5 GHz based on (10 dB criterion).

The slight variation in measured results between Ant1 and Ant5 due to imperfect fabrication or soldering. Whereas the ports isolation is better than 13 dB for any two antennas for the proposed multiple antenna system. For brevity and clear representation and due to the symmetric configuration, some isolation curves (scattering parameters) are better than 20 dB within the operating band and are not given in Fig. 8. The antenna efficiency is about 60-50% with the corresponding peak realized a gain of 2.3 dBi for Ant1 and for Ant3. Whereas for Ant2 and Ant4, it varied in the interval of 57 to 50 % with a corresponding gain of 1.98 dBi, as plotted in Fig. 9.

A. MEASURED RADIATION PATTERNS

The 2-D far-field measurements are carried out in anechoic chamber. The directive power radiation pattern for the multiple slot antenna system is given for Ant1 and Ant5 at

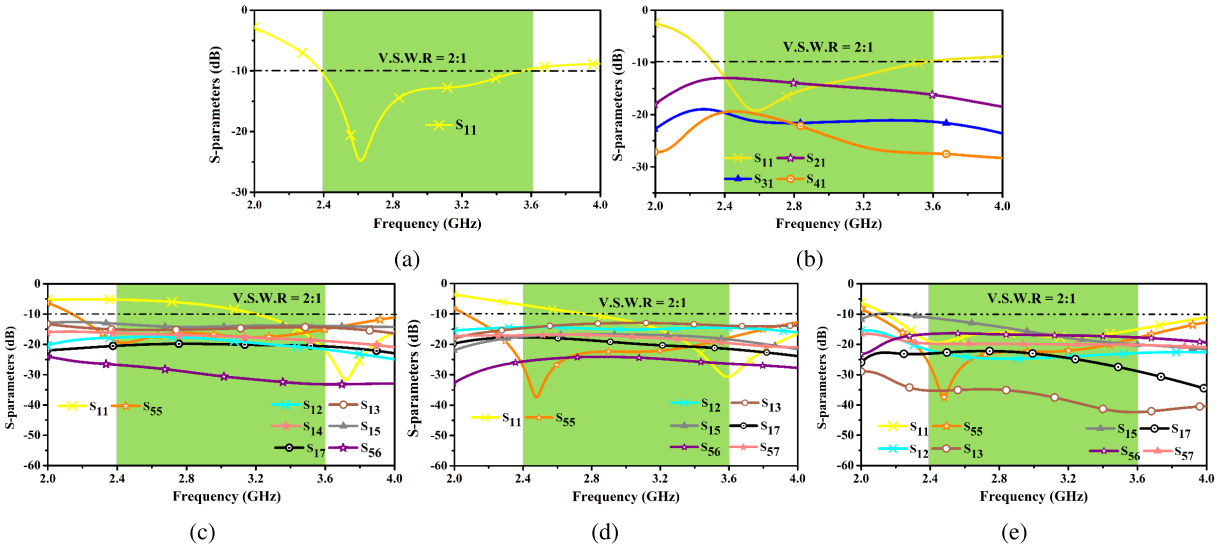

FIGURE 5. Simulated S-parameters (a) Single unit slot antenna (b) Four slot antennas etched at the corner of the ground plane (c) Case-1 different combination of rectangular slot antenna with vertical mounted open-end slot antenna (d) Case-2 (e) Proposed multiple slot antenna system.

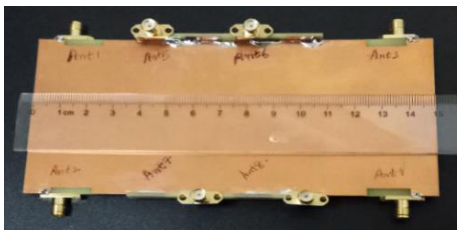

FIGURE 6. Fabricated prototype of proposed multiple input multiple output (MIMO) slot antenna array.

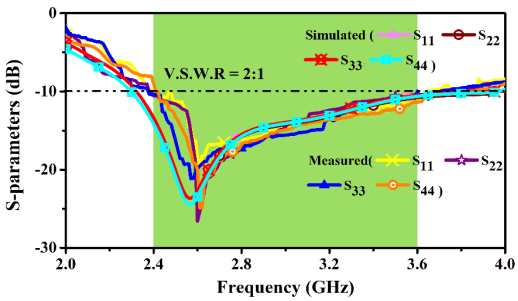

FIGURE 7. S-Parameters (impedance bandwidth).

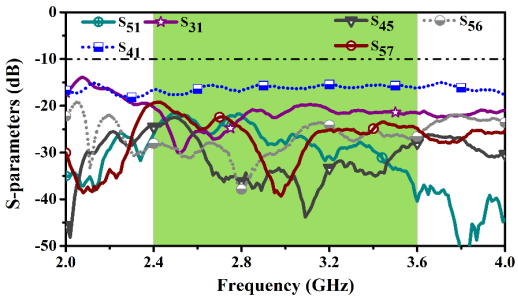

FIGURE 8. S-Parameters (measured port isolation).

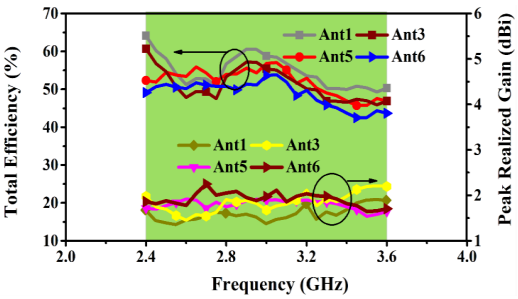

FIGURE 9. Measured total efficiency with peak realized gain.

2.6 GHz obtained from simulation and measured results. As with symmetric configuration, the Ant1 and Ant5 radiation patterns are selected for analysis of directive power gain. Furthermore, the radiation pattern covers the complementary space regions, result in pattern diversity. The simulated and measured radiation pattern is shown in Fig. 10 for $\phi = 0°$ and $\phi = 90°$ plane.

B. MIMO PERFORMANCE

The important MIMO performance metrics such as envelope correlation coefficient (ECC) [Equation. (1)] and Mean effective gain (MEG) [Equation. (2)] are computed based on the assumption stated in [19], [20]. The minimum ECC required for optimal MIMO performance should be less than 0.5 [21], [22]. The calculated ECC for any two antenna is less than 0.2 and is plotted in Fig. 12. For optimal diversity performance with good channel characteristics and to satisfy the balance power criteria The MEGs calculated for all eight antenna elements are given in Table. 1. Based on the measured results of 2-D far-field and meet the required standard of MEGi≈MEGj. The MIMO channel capacity is calculated based on stated conditions reported in [23], and for the proposed MIMO antenna array, the measured channel capacity is 34.54 bps/Hz. Furthermore, customer hand effect

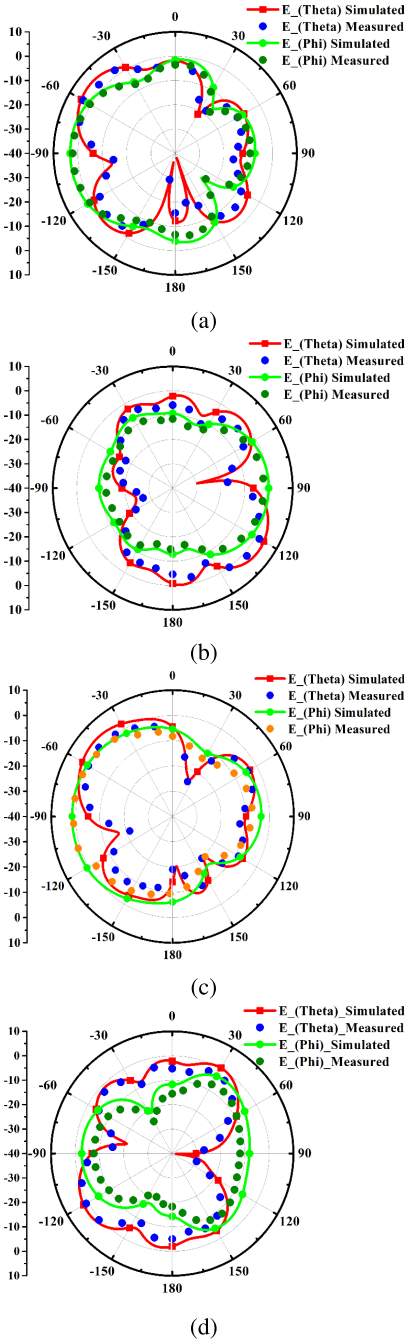

FIGURE 10. Measured radiation pattern for multiple slot antenna system for (a) Ant1, (b) Ant3, (c) Ant5 and (d) Ant6.

on ECC and MIMO channel capacity are studied and the reduction of channel capacity in customer hand scenario is due to reduction of antenna efficiency [24].

$$ECC = \frac{|\iint_{4\pi}(\vec{M}_i(\theta,\phi)) \times (\vec{M}_j(\theta,\phi))\, d\Omega|^2}{\iint_{4\pi}|(\vec{M}_i(\theta,\phi))|^2\, d\Omega \iint_{4\pi}|(\vec{M}_j(\theta,\phi))|^2\, d\Omega} \quad (1)$$

where $\vec{M}_i(\theta,\phi)$ describe the 3D radiation pattern when antenna i is excited and $\vec{M}_j(\theta,\phi)$ describe the 3D radiation pattern when antenna j is excited. The solid angle in the above

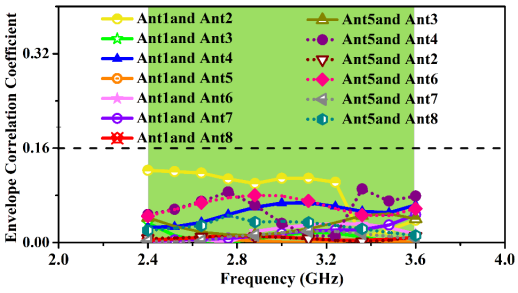

FIGURE 11. Envelope correlation coefficient.

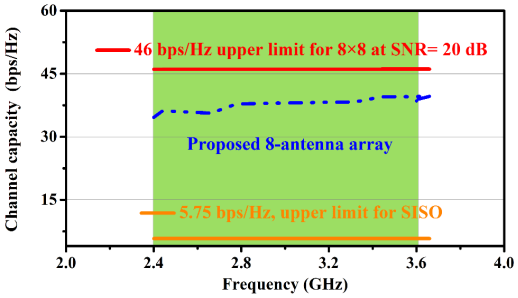

FIGURE 12. Calculated erogodic channel capacities of the fabrication multiple slot antenna system.

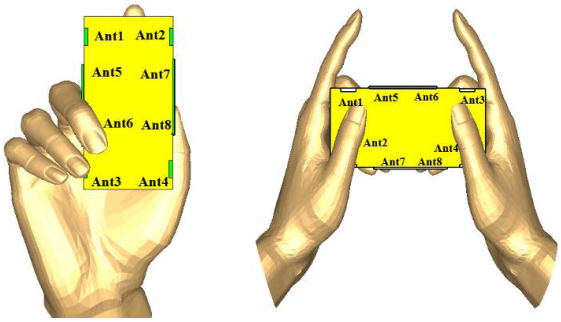

FIGURE 13. Customer hand effect for the multiple slot antenna system (a) Single Hand use (SHO) (b) Two hand Use (THO) (Right Hand is considered).

equation (1) is represented as Ω.

$$MEG = \int_{-\pi}^{\pi}\int_{0}^{\pi}[\frac{r}{r+1}G_\theta(\theta,\phi)P_\theta(\theta,\phi) + \frac{1}{1+r}G_\phi(\theta,\phi)P_\phi(\theta,\phi)]sin\theta d\theta d\phi \quad (2)$$

where $G_\phi(\theta,\phi)$ and $P_\theta(\theta,\phi)$ are angle of arrival and r is the cross polar ratio which can be expressed as Equation. (3).

$$r = 10log_{10}(\frac{P_{vpa}}{P_{hpa}}) \quad (3)$$

where the power received by vertically polarized antenna and horizontally polarized antenna is represented as P_{vpa} and P_{hpa}, respectively.

TABLE 1. MEG for Ant1 to Ant8.

Frequency	MEG_1 (dB)	MEG_2 (dB)	MEG_3 (dB)	MEG_4 (dB)	MEG_5 (dB)	MEG_6 (dB)	MEG_7 (dB)	MEG_8 (dB)
2.6 GHz	-3.13	-3.12	-3.10	-3.19	-2.8	-2.43	-2.79	-2.85
Indoor	-5.70	-5.87	-4.58	-5.43	-6.50	-6.81	-6.90	-6.60

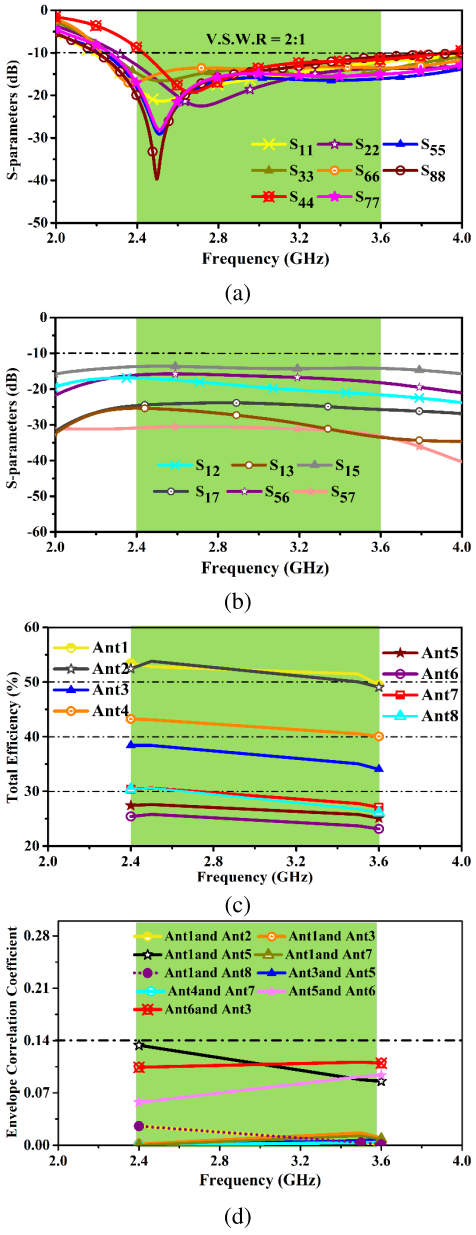

FIGURE 14. (a) S-Parameters (reflection co-efficient in SHO Mode) (b) Port isolation in SHO mode (c) Antenna efficiency in SHO mode (d) Envelop correlation coefficient in SHO mode.

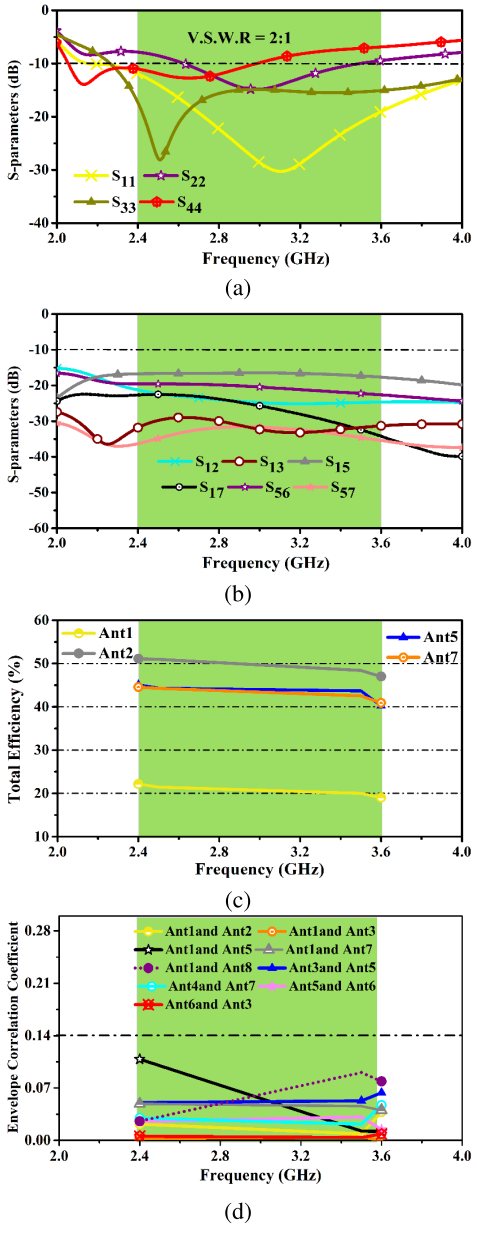

FIGURE 15. (a) S-Parameters (reflection co-efficient in THO Mode) (b) Port isolation in THO mode (c) Antenna efficiency in THO mode (d) Envelop correlation coefficient in THO mode.

VI. CUSTOMER HAND EFFECT

The customer hand or human hand effect on the multiple antenna array to mimic the use of mobile phone customer is studied in this section. As predicting, the performance of different usage positions is impossible, the only data-mode operation is considered for this study. It can be further classified as Single Hand Operation (SHO) and Two-Hand Operation (THO) as shown in Fig. 13. The desired antenna performance metrics including S-parameters, total efficiencies and diversity measures such as envelope correlation coefficient for SHO and THO is presented in this section.

TABLE 2. Performance comparison Smartphone antenna. Abbreviation: Number of Antenna elements = # Ant, Antenna Efficiency = Ant %, Peak Channel Capacity (bps/Hz) = PCC, Envelope correlation Coefficient = ECC, Not Given = NG.

Ref.	Bandwidth (GHz)	#Ant	Ant % (meas)	PCC	ECC
[11]	3.3–3.6 (-10 dB)	8	40–60	37	<0.15
[12]	3.4–3.6 (-10 dB)	8	44–55	36	0.10
[13]	3.4–3.6 (-10 dB)	8	62–76	40	0.05
[14]	1.8–1.9/ 2.3–2.6 (-10 dB)	6	37–79	NG	0.16
[15]	3.4–3.6 (-10 dB)	8	45–58	37	0.1
[16]	3.4–3.6 (-10 dB)	12	50–68	57	0.2
[17]	3.4–3.6 (-10 dB)	8	62–78	39	0.2
[7]	3.4–3.6 (-6 dB)	8	30–52	37	0.3
[5]	2.55–2.65 (-10 dB)	8	48–63	40	0.15
[6]	2.55–2.65 (-10 dB)	8	48–58	39	0.2
This Work	2.5–3.6 (-10 dB)	8	45–65	34.25	<0.02

By introduction of customer hand leads to dielectric loading of the proposed eight antenna array, affecting the performance, by absorbing radiating power in the near-field region result in the reduction of antenna efficiency as discussed in [24]–[26].

For SHO, the S parameters depicted in Fig. 14a reveals resonance shift for Ant6, due to lossy hand phantom correspondingly the total efficiency of antennas (Ant5, Ant6, Ant7, and Ant8). Under SHO, the port isolation in Fig. 14b are well below −10 dB. The (Ant1, Ant2, Ant3, Ant4) exhibit good radiation efficiency, resulted in better total efficiency which can be seen in Fig. 15c. Fig. 15d shows the ECC for any two-antenna element of the multiple antenna system is well below than 0.1.

The corresponding antenna efficiency for the SHO is given in Fig. 14c. According to SHO mode, the palm is near a smartphone, because of the efficiency for Ant5 to Ant8 less than 32% with Ant6 and Ant8 less than 25% due to close proximity. Furthermore, Ant1 and Ant2 are less affected with efficiency less than 52%.

In THO the thumbs are in close positioned along the short edges, right over the metal frame. There is minimum separation distance of 10 mm. And the extreme position antenna elements such as (Ant1, Ant2, Ant3, and Ant4) are completely covered. As with symmetric condition (Ant1, Ant2, Ant3, Ant4) performance is discussed. For antenna closer to the index finger (Ant1 and Ant3) the total efficiency is greater than 30 %.Thus, the proposed multiple antenna system is promising for massive MIMO operation under THO with application for 5G mobile terminal.

Recently, different techniques have been proposed to mitigate the user hand effect. According to [27], a thick buffer material with high permittivity or dielectric constant with low loss or low conductivity used. Such material can be helpful to counter the near-field coupling of the radiating antenna with hand. This technique needs extra volume. Furthermore, in [28] dynamically selecting the antenna with the best performance metrics in the presence of user hand for a mobile terminal. Aside from the above-mentioned techniques, the user hand effect mitigated by using passive circuit components or tuning circuit classified as adaptive impedance matching (AIM) [28]. The AIM is a separate circuit module attached to the antenna with variable impedance to detect the time varying mismatch such as user'. This work studied the direct interaction of the antenna array with the user hand and the method discussed in [27], [28] can be adopted to reduce the effect of user hand dielectric loading of the proposed antenna array. Table 2 shows the performance comparison between the proposed works and the previous report. We can see that our proposed antenna has better performance in terms of operating bandwidth and ECC.

VII. CONCLUSION

An eight-slot antenna array for MIMO operation is presented to be adopted for a 5G smartphone at 2.6 GHz and 3.5 GHz. Each antenna operates in the desired frequency band of operation (2.4 GHz - 3.6 GHz) with the minimum acceptable isolation of (≤ -15 dB) and ECC less than 0.2 for any two antennas of the array. The calculated ergodic MIMO channel capacity for 8×8 MIMO based for the proposed MIMO antenna array based on measured was approximately 34.54 bps/Hz with 20 dB as reference SNR in free space scenario. It was 3 times larger relative to 2×2 MIMO antenna systems capacity of 11.5 bps/Hz.

REFERENCES

[1] S. Malkowsky, J. Vieira, L. Liu, P. Harris, K. Nieman, N. Kundargi, I. C. Wong, F. Tufvesson, and V. Öwall, and O. Edfors, "The world's first real-time testbed for massive MIMO: Design, implementation, and validation," *IEEE Access*, vol. 5, pp. 9073–9088, 2017.

[2] L. Malviya, R. K. Panigrahi, and M. Kartikeyan, "MIMO antennas with diversity and mutual coupling reduction techniques: A review," *Int. J. Microw. Wireless Technol.*, vol. 9, no. 8, pp. 1763–1780, 2017.

[3] T. Wang, G. Li, J. Ding, Q. Miao, J. Li, and Y. Wang, "5G spectrum: Is China ready?" *IEEE Commun. Mag.*, vol. 53, no. 7, pp. 58–65, Jul. 2015.

[4] K. Takahashi, N. Honma, K. Murata, and Y. Tsunekawa, "Miniaturized six port MIMO antenna using T-shaped conductor and reactance-loaded notch antenna," *IEICE Commun. Express*, vol. 5, no. 2, pp. 57–62, 2016.

[5] M.-Y. Li, Y.-L. Ban, Z.-Q. Xu, G. Wu, K. Kang, and Z.-F. Yu, "Eight-port orthogonally dual-polarized antenna array for 5G smartphone applications," *IEEE Trans. Antennas Propag.*, vol. 64, no. 9, pp. 3820–3830, Sep. 2016.

[6] M.-Y. Li, Z.-Q. Xu, Y.-L. Ban, C.-Y.-D. Sim, and Z.-F. Yu, "Eight-port orthogonally dual-polarised MIMO antennas using loop structures for 5G smartphone," *IET Microw., Antennas Propag.*, vol. 11, no. 12, pp. 1810–1816, 2017.

[7] K.-L. Wong, J.-Y. Lu, L.-Y. Chen, W.-Y. Li, and Y.-L. Ban, "8-antenna and 16-antenna arrays using the quad-antenna linear array as a building block for the 3.5-GHz LTE MIMO operation in the smartphone," *Microw. Opt. Technol. Lett.*, vol. 58, no. 1, pp. 174–181, Jan. 2016.

[8] D.-J. Lee, S.-J. Lee, S.-T. Khang, and J.-W. Yu, "Extensible compact 8-port MIMO antenna with pattern gain," *Microw. Opt. Technol. Lett.*, vol. 59, no. 2, pp. 236–240, 2017.
[9] K.-L. Wong and J. Y. Lu, "3.6-GHz 10-antenna array for MIMO operation in the smartphone," *Microw. Opt. Technol. Lett.*, vol. 57, no. 7, pp. 1699–1704, Jul. 2015.
[10] A. Iqbal, A. Smida, N. K. Mallat, R. Ghayoula, I. Elfergani, J. Rodriguez, and S. Kim, "Frequency and pattern reconfigurable antenna for emerging wireless communication systems," *Electronics*, vol. 8, no. 4, p. 407, 2019.
[11] W. Jiang, B. Liu, Y. Cui, and W. Hu, "High-isolation eight-element MIMO array for 5G smartphone applications," *IEEE Access*, vol. 7, pp. 34104–34112, 2019.
[12] K.-L. Wong, C.-Y. Tsai, and J.-Y. Lu, "Two asymmetrically mirrored gap-coupled loop antennas as a compact building block for eight-antenna MIMO array in the future smartphone," *IEEE Trans. Antennas Propag.*, vol. 65, no. 4, pp. 1765–1778, Apr. 2017.
[13] Y. Li, C.-Y.-D. Sim, Y. Luo, and G. Yang, "High-isolation 3.5 GHz eight-antenna MIMO array using balanced open-slot antenna element for 5G smartphones," *IEEE Trans. Antennas Propag.*, vol. 67, no. 6, pp. 3820–3830, Jun. 2019.
[14] Z. Chen, W. Geyi, M. Zhang, and J. Wang, "A study of antenna system for high order MIMO device," *Int. J. Antennas Propag.*, vol. 2016, Feb. 2016, Art. no. 1936797.
[15] M. S. Sharawi, M. A. Jan, and D. N. Aloi, "Four-shaped 2 × 2 multi-standard compact multiple-input–multiple-output antenna system for long-term evolution mobile handsets," *IET Microw., Antennas Propag.*, vol. 6, no. 6, pp. 685–696, 2012.
[16] M.-Y. Li, Y.-L. Ban, Z.-Q. Xu, J. Guo, and Z.-F. Yu, "Tri-polarized 12-antenna MIMO array for future 5G smartphone applications," *IEEE Access*, vol. 6, pp. 6160–6170, Dec. 2017.
[17] Y.-L. Ban, C. Li, C.-Y.-D. Sim, G. Wu, and K.-L. Wong, "4G/5G multiple antennas for future multi-mode smartphone applications," *IEEE Access*, vol. 4, pp. 2981–2988, 2016.
[18] N. Behdad and K. Sarabandi, "A multiresonant single-element wideband slot antenna," *IEEE Antennas Wireless Propag. Lett.*, vol. 3, no. 1, pp. 5–8, Dec. 2004.
[19] A. Iqbal, O. A. Saraereh, A. Bouazizi, and A. Basir, "Metamaterial-based highly isolated MIMO antenna for portable wireless applications," *Electronics*, vol. 7, no. 10, p. 267, 2018.
[20] Y. Ding, Z. Du, K. Gong, and Z. Feng, "A novel dual-band printed diversity antenna for mobile terminals," *IEEE Trans. Antennas Propag.*, vol. 55, no. 7, pp. 2088–2096, Jul. 2007.
[21] A. Iqbal, O. A. Saraereh, A. W. Ahmad, and S. Bashir, "Mutual coupling reduction using F-shaped stubs in UWB-MIMO antenna," *IEEE Access.*, vol. 6, pp. 2755–2759, 2018.
[22] A. Iqbal, A. Basir, A. Smida, N. K. Mallat, I. Elfergani, J. Rodriguez, and S. Kim, "Electromagnetic bandgap backed millimeter-wave MIMO antenna for wearable applications," *IEEE Access*, vol. 7, pp. 111135–111144, 2019.
[23] P.-S. Kildal and K. Rosengren, "Correlation and capacity of MIMO systems and mutual coupling, radiation efficiency, and diversity gain of their antennas: Simulations and measurements in a reverberation chamber," *IEEE Commun. Mag.*, vol. 42, no. 12, pp. 104–112, Dec. 2004.
[24] V. Plicanic, B. K. Lau, and Z. Ying, "Performance of a multiband diversity antenna with hand effects," in *Proc. Int. Workshop Antenna Technol., Small Antennas Novel Metamater.*, Mar. 2008, pp. 534–537.
[25] S. S. Zhekov, A. Tatomirescu, E. Foroozanfard, and G. F. Pedersen, "Experimental investigation on the effect of user's hand proximity on a compact ultrawideband MIMO antenna array," *IET Microw. Antennas Propag.*, vol. 10, no. 13, pp. 1402–1410, 2016.
[26] M. Pelosi, O. Franek, M. B. Knudsen, G. F. Pedersen, and J. B. Andersen, "Antenna proximity effects for talk and data modes in mobile phones," *IEEE Antennas Propag. Mag.*, vol. 52, no. 3, pp. 15–27, Jun. 2010.
[27] M. Pelosi, O. Franek, M. B. Knudsen, and G. F. Pedersen, "Influence of dielectric loading on PIFA antennas in close proximity to user's body," *Electron. Lett.*, vol. 45, no. 5, pp. 246–248, 2009.
[28] I. Vasilev, V. Plicanic, and B. K. Lau, "On user effect compensation of MIMO terminals with adaptive impedance matching," in *Proc. IEEE Antennas Propag. Soc. Int. Symp. (APSURSI)*, Jul. 2013, pp. 174–175.

MUJEEB ABDULLAH received the bachelor's degree from the University of Engineering and Technology (UET) at Mardan, Mardan, in 2007, the master's degree in electrical engineering with a focus on telecommunication from the Blekinge Institute of Technology, Sweden, in 2011, and the Ph.D. degree from the University of Electronic Science and Technology (UESTC) of China, China, in 2018. He is currently an Assistant Professor with Bacha Khan University, Charsadda, Pakistan. His research interests include MIMO antenna array, 5G mobile terminals, wearable antennas, and multiband antennas.

SAAD HASSAN KIANI received the bachelor's degree in electrical engineering from the City University of Science and Information Technology, Peshawar, Pakistan, in 2014, and the master's degree from Iqra National University, Peshawar, in 2018. He is currently a Visiting Lecturer with the Electrical Engineering Department, Iqra National University, and Abasyn University, Peshawar. His research interests include MIMO antenna array, 5G mobile terminals, wearable antennas, and multiband antennas.

AMJAD IQBAL (S'18) received the degree in electrical (telecommunication) engineering from the COMSATS Institute of Information Technology, Islamabad, Pakistan, in 2012, and the M.S. degree in electrical engineering from the Department of Electrical Engineering, CECOS University of IT and Emerging Sciences, Peshawar, Pakistan, in 2018. He is currently pursuing the Ph.D. degree with the Faculty of Engineering, Multimedia University, Cyberjaya, Malaysia. He was a Lab Engineer with the Department of Electrical Engineering, CECOS University, from 2016 to 2018. His research interests include printed antennas, flexible antennas, implantable antennas, MIMO antennas, dielectric resonator antennas, and synthesis of microwave components.